JOURNAL OF Applied Polymer SCIENCE

Special Issue: Sustainable Polymers and Polymer Science Dedicated to the Life and Work of Richard P. Wool

Guest Editors: Dr Joseph F. Stanzione III (Rowan University, U.S.A.)
and Dr John J. La Scala (U.S. Army Research Laboratory, U.S.A.)

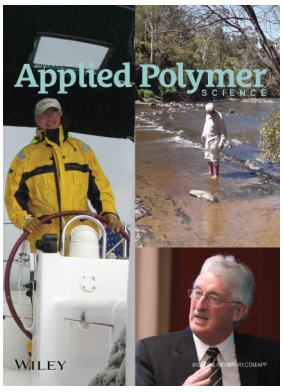

EDITORIAL

REVIEWS

RESEARCH ARTICLES

JOURNAL OF Applied Polymer SCIENCE

Special Issue: Sustainable Polymers and Polymer Science Dedicated to the Life and Work of Richard P. Wool

Guest Editors: Dr Joseph F. Stanzione III (Rowan University, U.S.A.)
and Dr John J. La Scala (U.S. Army Research Laboratory, U.S.A.)

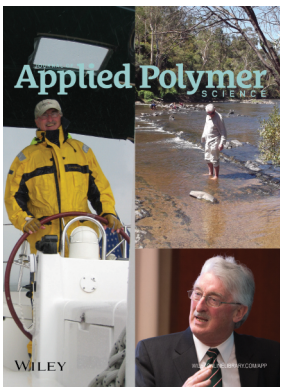

Journal of Applied Polymer Science

Physical aging and mechanical performance of poly(L-lactide)/ZnO nanocomposites

Erlantz Lizundia,[1] Leyre Pérez-Álvarez,[1,3] Míriam Sáenz-Pérez,[1,2] David Patrocinio,[1] José Luis Vilas,[1,3] Luis Manuel León[1,3]

[1]Macromolecular Chemistry Research Group (LABQUIMAC), Department of Physical Chemistry, Faculty of Science and Technology, University of the Basque Country (UPV/EHU), Leioa 48940 Spain

[2]The Footwear Technology Center of La Rioja, Calle Raposal 65, Arnedo 26580, Spain

[3]Basque Center for Materials, Applications and Nanostructures (BCMaterials), Parque Tecnológico de Bizkaia, Ed. 500, Derio 48160, Spain

Correspondence to: E. Lizundia (E-mail: erlantz.liizundia@ehu.eus)

ABSTRACT: In this work nanocomposites based on poly (L-lactide) (PLLA) and zinc oxide (ZnO) nanoparticles with a concentration up to 5 wt % have been prepared by solvent-precipitation followed by compression moulding at 200 °C. Structural evolution of nanocomposites as a function of time and nanoparticle concentration has been monitored by differential scanning calorimetry (DSC). Results reveal a marked reduction of the enthalpy relaxation rate β_H from 3.273 J/g for neat polymer to 0.912 J/g for its 0.25 wt % reinforced counterpart, revealing slower aging dynamics induced by zinc oxide. It is shown by field emission scanning electron microscopy (FE-SEM) that concentrations larger than 1 wt % yield nanoparticle agglomeration. These large aggregates decrease the amount of nanoparticle surfaces exposed to PLLA chains, notably reducing the efficiency of ZnO nanoparticles to delay the physical aging of its hosting matrix. Mechanical tests show an increased stiffness upon ZnO loading as denoted by the increase in modulus from 2310 MPa to 2780 MPa for the 1 wt % nanocomposite. Obtained findings through this work lead the way for the development of nanocomposites based on renewable polymers and natural fillers to be used in packaging applications, where the use of nonbiodegradable materials for short-term applications is extended. © 2016 Wiley Periodicals, Inc. J. Appl. Polym. Sci. **2016**, *133*, 43619.

KEYWORDS: composites; glass transition; mechanical properties; nanoparticles; nanowires and nanocrystals; packaging

Received 24 December 2015; accepted 9 March 2016
DOI: 10.1002/app.43619

INTRODUCTION

Currently, most of the commonly utilized polymers are derived from petrochemical resources, which represent serious environmental problems because of the increasing challenge arising from the oil-depletion. Moreover, those petro-based materials are mainly nonbiodegradable and are not always easy to recycle. A plausible solution to overcome those aspects would arise from the use of materials based on renewable resources. In this trend of obtaining sustainable materials, becomes essential the development of bio-based materials for packaging applications, where the use of nonbiodegradable plastics for short-term uses is very widespread.

In this framework, the family of polylactides emerges as one of the most promising bio-based materials because of their economically feasible industrial production, good biocompatibility, low cost, printability, and high optical transmittance.[1,2] Among all the different isomeric forms of polylactides, the semicrystalline poly (L-lactide) (PLLA) could be viewed as the most interesting one because it is easily tuneable phase-structure and mechanical properties.[3] Additionally, this thermoplastic material fulfils many requirements of the traditional nonbiodegradable packaging materials. Unfortunately, due to its relatively low glass transition temperature of about 55−65 °C depending on the crystalline fraction developed during processing,[4] PLLA undergoes a considerable physical aging when is used at ambient temperature, which notably limits its use as commodity plastic.

More precisely, the cooling of a polymer from the melt to temperatures below T_g yields a nonequilibrium state. This metastable glassy material has higher specific volume, enthalpy and entropy than the polymer in its corresponding equilibrium state. The thermodynamic equilibrium is reached by means of a

Additional Supporting Information may be found in the online version of this article.

rearrangement of macromolecules to modify their conformation. This process in which a new structure is achieved is often referred as physical aging.[5,6] During this structure evolution, the macroscopic properties such as tensile modulus, brittleness and gas permeability could be drastically modified, which limits the stability of polymeric materials during their use inasmuch as obtained macroscopic properties are time-dependant.[7–9]

Up to date considerable efforts have been made to understand the physical aging mechanism of neat polymers such as poly (methyl methacrylate) (PMMA), poly(vinyl acetate) (PVAc), polylactide (PLA), or poly (ethylene terephthalate) (PET).[10–14] In this framework, some authors have found that the inclusion of nano-reinforcements into polymeric materials reduces the physical aging of bulk nanocomposites.[15,16] In fact, Priestley *et al.* have proven by monitoring fluorescence in multilayer films that the rate of structural relaxation of PMMA is reduced by a factor of 15 at the substrate interface.[17] Thus, it may be hypothesized that nanocomposite approach would result an efficient strategy to face this matter.

Accordingly, the introduction of well-dispersed nanoparticles having a large surface area to volume ratio would reduce the physical aging of the hosting polymeric matrix to a larger extent than spherical nanoparticles. To that end, rod-shaped nanoparticles would provide large interfacial areas in which the conformational changes of PLLA would be limited. Among all the available nanoparticles, zinc oxide (ZnO) nanoparticles are of special interest because of their outstanding mechanical properties, large surface to volume ratio, biocompatibility, green character, and low cost.[18] Indeed, it has been proven that the introduction of ZnO nanoparticles improves several functional properties of biopolymers such as the UV-permeability, thermal stability, surface hydrophobicity, and mechanical properties.[19,20]

In this work ecologically friendly PLLA/ZnO materials are developed in an attempt to reduce the conformational changes leading to physical aging of PLLA. Obtained results reveal that incorporated ZnO-PLLA interfacial areas successfully reduce the conformational changes occurring in PLLA, which represents a step forward for the establishment of a sustainable society.

EXPERIMENTAL

Starting Materials

PLLA of number-average molecular weight (M_n) 100,000 g/mol and a polydispersity index (M_w/M_n) of 1.85 kindly supplied by Purac Biochem (The Netherlands) has been used as a matrix. 43 ± 24 nm long and ~13 nm wide rod-shaped zinc oxide (ZnO) nanoparticles have been purchased by ÚUrederra technological centre (Spain). Chloroform and methanol were purchased by Panreac.

Sample Preparation

Nanocomposites have been prepared by solvent-precipitation followed by compression moulding as described previously.[19] Briefly, ZnO was homogeneously dispersed in chloroform ($CHCl_3$) via mild sonication in a Vibra-CellTM CV 334 ultrasonic processor. Then, the required amount of previously dissolved PLLA in chloroform was added to obtain nanocomposites with a concentration ranging from 0.25 to 5 wt %. Dispersions were were submitted to an additional sonication step for 5 min and they were subsequently precipitated in an excess of cold methanol. After drying the resulting materials for 48 h at 60 °C in a vacuum oven, nanocomposites were conformed as sheets with thickness of 400 μm sheets with thickness compression moulding at 200 °C (below the onset temperature of thermodegradation; see Supporting Information, Figure S1) for 4 min with a pressure of 150 MPa and subsequent solidification by water quenching. In this way, quick cooling of composites below the T_g was assured, preventing any further development of crystallinity.

Differential Scanning Calorimetry (DSC)

Physical aging of nanocomposites was determined using a Mettler Toledo DSC 822e calorimeter under nitrogen atmosphere (30 mL/min). Aged samples (at 40 °C in an oven for different times) were sealed in an aluminium pan and they were heated from −20 °C to 200 °C at a rate of 10 °C/min. Moreover, the PLLA crystalline fraction X_c (%) attributable was determined to ensure that no crystallization takes place during the physical aging process[4]:

$$X_c(\%) = \frac{\Delta H_f - \Delta H_c}{\Delta H_f^0} \cdot 100 \quad (1)$$

where ΔH_f and ΔH_c are respectively the enthalpy of fusion and cold crystallization of the samples determined on the DSC. $\Delta H_f^0 = 93$ J/g was taken as the heat of fusion of an infinitely thick PLLA crystal.[22]

Field Emission Scanning Electron Microscopy (FE-SEM)

ZnO nanoparticle dispersion within the PLLA has been analyzed using a Hitachi S-4800 field emission scanning electron microscope (FE-SEM) at an acceleration voltage of 5 kV. Cryogenically fractures surfaces have been copper-coated in a Quorum Q150T ES turbo-pumped sputter coater (5 nm thick coating).

Tensile Testing

The mechanical performance of PLLA/ZnO nanocomposites has been evaluated by tensile testing. Specimens were punched out from films according to ISO 527-1:2012 and they were conditioned at 22 °C and 51%RH for overnight before their characterization. Experiments were carried out on a AGS-X Universal Testing Machine from Shimadzu at 5mm/min. Young's modulus (E), stress and strain at yield (σ_y and ε_y respectively) and stress and strain at break (σ_r and ε_r respectively) were determined. Reported values represent mean average value and standard deviation over five specimens.

Dynamic Mechanical Analysis (DMA)

DMA was performed on a DMA/SDTA861 analyzer (Mettler-Toledo) in tensile mode. 200 μm thick, 4 mm wide and 5 mm long specimens were submitted to displacement sweeps at 1 Hz and 0 °C. Moreover, curves displaying the energy loss (tan δ) were recorded as a function of temperature at a heating rate of 3 °C/min, a frequency of 1 Hz and displacement of 3 μm.

RESULTS AND DISCUSSION

Physical Aging

It has been reported in the literature that the physical aging of semicrystalline polymers such as PLLA depends on the relative

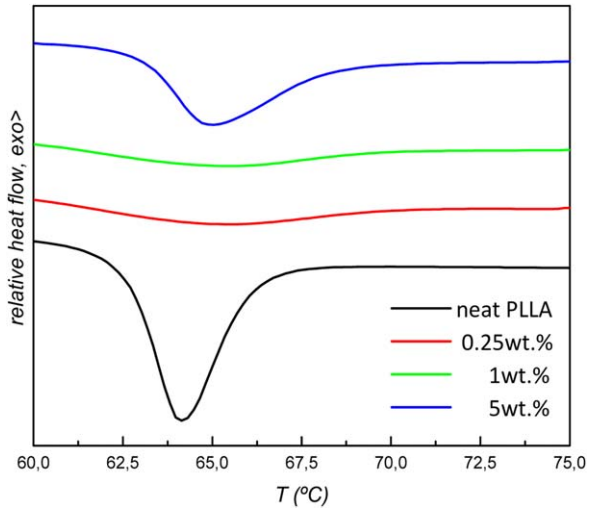

Figure 1. DSC heating scan at T_g region for nanocomposites aged during 162 h. [Color figure can be viewed in the online issue, which is available at wileyonlinelibrary.com.]

amount of crystalline/amorphous phase.[10,14] To that end, the possible crystallization of nanocomposites was prevented by water quenching treatment. Performed DSC experiments after compression moulding (Supporting Information, Figure S2) reveal that both glass transition temperature (T_g) and melting temperature (T_m) remain unchanged for all the compositions, indicating that no chain scission event occurred during the fabrication of the nanocomposites. Furthermore, to ensure that structural changes are only due to the restriction effects of zinc oxide nanoparticles on the segmental motion of PLLA the crystalline fraction of nanocomposites has been calculated according to eq. (1). Results reveal that X_c remains nearly constant at 8% upon aging (see DSC traces provided in Supporting Information, Figure S3), which agrees well with the model proposed by Struik as those aging experiments were carried out well below the glass transition temperature of nanocomposites (region I in Struiḱs model).[21]

Differential scanning calorimetry experiments of physically aged specimens at 40 °C (16 °C below T_g) for different times have been carried out in order to elucidate how structural relaxation proceeds in PLLA/ZnO nanocomposites. For clarity purposes, Figure 1 only shows the DSC heating scans of specimens aged for 162 h, although nanocomposites have been aged up to 300 h. It is shown that all the aged nanocomposites present a noticeable endothermic overshoot at the T_g, which is not observed for non-aged materials. More precisely, the area under the endothermic overshoot sharply decreases with the addition of 0.25 and 1 wt % ZnO, although larger concentrations yield comparable δ_H enthalpy relaxation (calculated by subtracting the enthalpy relaxation of the non-aged curve) to that corresponding to pure PLLA. Additionally, longer aging times (not shown) systematically increase the enthalpy relaxation of composites. In fact, as polymer evolves towards equilibrium during aging process, more energy is required for the glass transition, resulting in a marked endothermic overshot at glass transition together with an increase of the T_g.[23]

Physical aging kinetics could be easily extracted from performed DSC experiments by accounting for the enthalpy relaxation change upon aging. In this framework, the enthalpy relaxation rate (β_H) could be quantified as:[24]

$$\beta_H = \left[\frac{\partial \delta_H}{\partial(\log t_a)}\right]_{q_1,q_2,T_a} \quad (2)$$

where q_1 and q_2 are the cooling and heating rates respectively and T_a and t_a are the aging temperature and time respectively. Obtained β_H values are then normalized with respect to the polymer fraction into the nanocomposite.

Figure 2 shows the enthalpy relaxation rate (β_H) of PLLA and its ZnO nanocomposites which gives us an insight about the chain segmental relaxation occurring in bulk material. Experimental results show a reduction of β_H values from 3.273 J/g for neat polymer to 0.912 J/g for its 0.25 wt % reinforced counterpart, which represents a 3.6-fold reduction. This slower aging dynamics induced by the presence of zinc oxide nanoparticles suggest that the presence of zinc oxide nanoparticles delays the ability of polymeric chains in their way to a metastable state closer to thermodynamic equilibrium. It may be noted that obtained physical aging reduction for such a low concentration of zinc oxide nanoparticles is much larger than that previously reported for poly (methyl methacrylate)/silica and polystyrene/gold nanocomposites.[10,25,26] Furthermore, Lin *et al.* found faster physical aging of polystyrene with the addition of 3 wt % silver nanoparticles.[27] They ascribed this behaviour to the weak polymer–nanoparticle interactions which cause a plasticizing effect on the structural relaxation of polystyrene.

In view to obtained experimental findings, it could be hypothesized that the presence of ZnO nanoparticles restricts the chain mobility of PLLA macromolecules at the nanoparticle-matrix interface, which in turn reduces the bulk physical aging rate of the nanocomposite. On the contrary, larger concentrations yield notably larger enthalpy relaxation rates. The existence of a critical concentration in which ZnO nanoparticles induce larger changes in the relaxation of polymeric chains may be ascribed

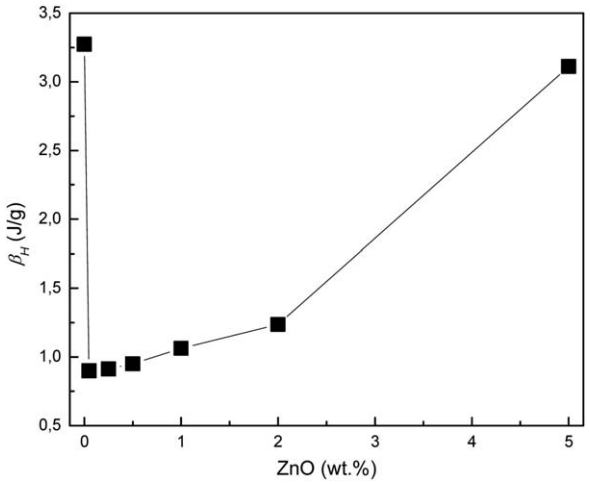

Figure 2. Enthalpy relaxation rate values depending on the ZnO concentration.

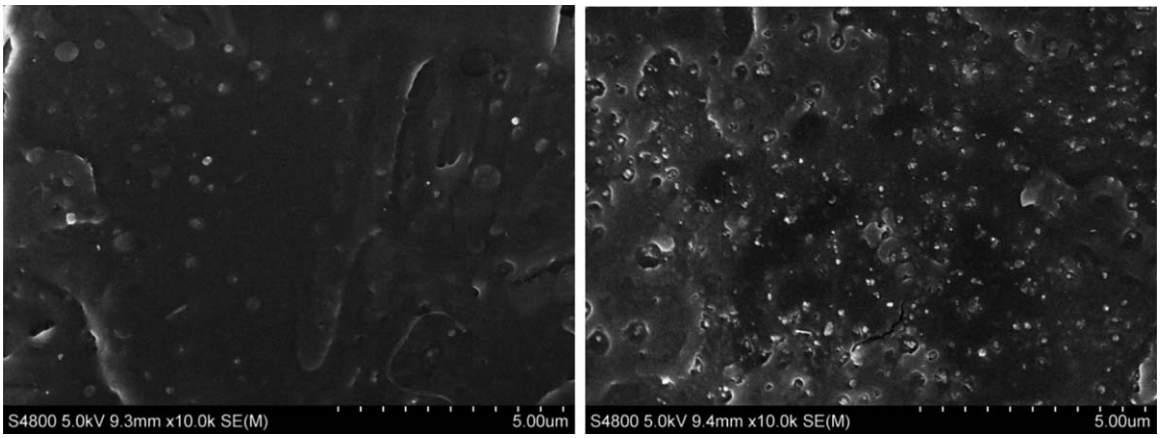

Figure 3. Representative FE-SEM micrographs showing ZnO dispersion within PLLA matrix for nanocomposites containing (a) 1 wt % and (b) 5 wt %.

to uneven distribution of nanoparticles within the matrix, as would be shown in the following section.

Morphological Evaluation

Field emission scanning electron microscopy (FE-SEM) has been carried out to obtain further insights on the dispersion of ZnO nanoparticles within the polymeric matrix. In this line, Figure 3 depicts representative FE-SEM micrographs for PLLA/ZnO nanocomposites containing 1 and 5 wt %. It could be observed that at a concentration of 1 wt % zinc oxide nanoparticles remain separated and they are well-distributed into the PLLA, while a marked nanoparticle aggregation occurs at a concentration of 5 wt % [Figure 3(b)]. Similar aggregation effects were obtained for several polylactide-based nanocomposites such as PLLA/MWCNT,[24] PLA/silicasol,[28] PLA/sepiolite, and PLA/ZnOs (silanized ZnO nanoparticles) nanocomposite systems.[29,30]

Those experimental findings allow us to better understand the occurring physical aging mechanism in PLLA/ZnO nanocomposites. It has been previously reported that the structural relaxation of polymeric chains is related to their relative distance from the interfaces.[17] More precisely, it has been found that the poly (methyl methacrylate) structural relaxation rate is reduced by a factor of 15 at the silica-polymer interface relative to bulk. This aging kinetic reduction extends up to ~200 nm from the interface. Thus, it could be expected that when ZnO nanoparticles remain well-dispersed, i.e., at concentrations up to 1 wt %, the large amount of ZnO-PLLA interfaces are enough to reduce the bulk physical aging by limiting the mobility of PLLA chains at the nanoparticle surface. On the contrary, at concentrations as high as 5 wt % the formation of large aggregates decreases the amount of available nanoparticle surfaces,[31] notably reducing the efficiency of these nanoparticles to delay the physical aging of bulk PLLA. Those results highlight the relevance of utilizing large surface area nanoparticles such as nanorods for the effective reduction of glassy-state physical aging in comparison with nanoparticles having spherical shapes.[32]

It is worthy to note that ZnO nanoparticles have been homogeneously dispersed by a simple solvent-precipitation/compression moulding method. On the opposite corner, Murariu et al. mixed silane-treated ZnO nanoparticles with PLLA.[33] They found that the addition of surface-treated zinc oxide nanoparticles results in an improved thermal stability and fine nanofiller dispersion, while thermal transitions are not affected. Although they notably improved some properties of PLLA, the fabrication of nanocomposites with well-dispersed nanoparticles using silane coupling agents would limit the prospective application of these materials because of the toxicity associated with silanes (some silanes produce methanol during their hydrolysis, which may be detrimental for tissue engineering applications for example).

Mechanical Performance

Due to the nanometric nature and the high tensile strength of ZnO particles, it would be expected that the stress transfer along the vast matrix-filler interfaces should greatly increase the modulus of the resulting composite. To that end, the static mechanical performance of nonaged PLLA/ZnO nanocomposites has been evaluated by means of uniaxial tensile testing.

Figure 4 shows the nominal stress−strain curves of neat PLLA and its nanocomposites, while Table I summarizes the main representative mechanical parameters of specimens under uniaxial tensile loading. As could be seen, neat PLLA shows a stiff

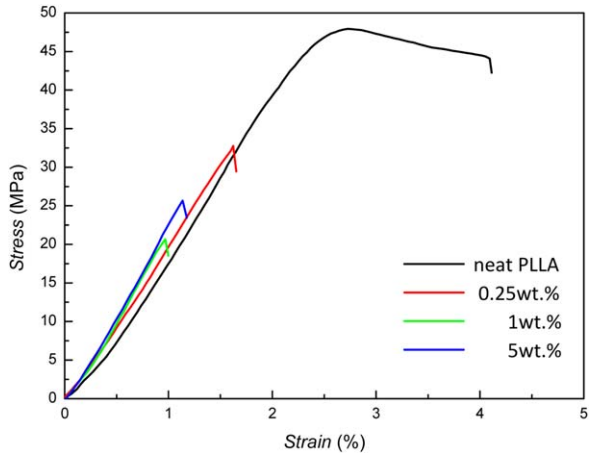

Figure 4. Stress−strain curves for neat PLLA and its ZnO nanocomposites. [Color figure can be viewed in the online issue, which is available at wileyonlinelibrary.com.]

Table I. Main Representative Mechanical Parameters for PLLA/ZnO Nanocomposites: Young's Modulus (E), Stress, and Strain at Yield (σ_y and ε_y, respectively) and Stress and Strain at Break (σ_b and ε_b, respectively)

ZnO (wt %)	E (MPa)	σ_y (MPa)	ε_y (%)	σ_b (MPa)	ε_b (%)
0	2309 ± 148	48.5 ± 3.9	2.45 ± 0.21	42.8 ± 3.2	4.57 ± 0.51
0.25	2589 ± 339	41.3 ± 10.3	1.66 ± 0.32	41.3 ± 10.3	1.68 ± 0.35
1	2776 ± 191	25.4 ± 7.1	1.02 ± 0.25	25.3 ± 7.1	1.02 ± 0.25
5	2743 ± 147	41.2 ± 7.7	1.23 ± 0.29	27.5 ± 5.2	1.23 ± 0.29

and semi-ductile behaviour as denoted by the strain at yield of 2.45% and fracture strain (ε_b) at 4.57%.[3] It is evidenced that specimens containing larger amounts of zinc oxide become stiffer as denoted by the increase in modulus from 2310 MPa to 2780 MPa for the 1 wt % nanocomposite, indicating that ZnO nanoparticles act as efficient reinforcing elements for mechanical stress. It is noticeable that the increase in stiffness is accompanied by a continuous increase in nanocomposite brittleness as demonstrated by the reduction of elongation at yield (ε_y) from 2.45% for neat polymer to 1.02% for its 1 wt % nanocomposite. This behavior may be ascribed to the incorporation of stress concentration areas with the addition of ZnO.

It is well established that the experimentally obtained tensile data could be compared with theoretical predictions by using Halpin-Tsai model,[34] which accounts for the longitudinal E modulus of composites composed by unidirectionally oriented fillers. In the case of randomly distributed fillers, the Youngs modulus of a composite could be estimated according to a modified Halpin-Tsai equation as:[35]

$$\frac{E_c}{E_m}=\left(\frac{3}{8}\right)\left(\frac{1+2\rho\eta_L\varphi_2}{1-\eta_L\varphi_2}\right)+\left(\frac{5}{8}\right)\left(\frac{1+2\rho\eta_T\varphi_2}{1-\eta_T\varphi_2}\right) \quad (3)$$

where E_c and E_m correspond to the Youngs moduli of the composite and matrix respectively, ρ is the aspect ratio of the filler (3 according to obtained TEM images) and ϕ_2 is its volume fraction. The volume fraction has been calculated assuming a density of 1.25 g/cm^3 for poorly crystalline PLLA and 5.606 g/cm^3 for ZnO wurtzite structure.[36] Moreover, η_L and η_T could be defined as:

$$\eta_L=\frac{E_r-1}{E_r+2\rho} \quad (4)$$

$$\eta_T=\frac{E_r-1}{E_r+2} \quad (5)$$

where E_r is defined as the ratio between the Youngs modulus of the filler and the matrix. The Young modulus of ZnO nanoparticles has been set at 75GPa according to the values obtained by atomic force microscopy, nanoindenter and optical interferometry.[37]

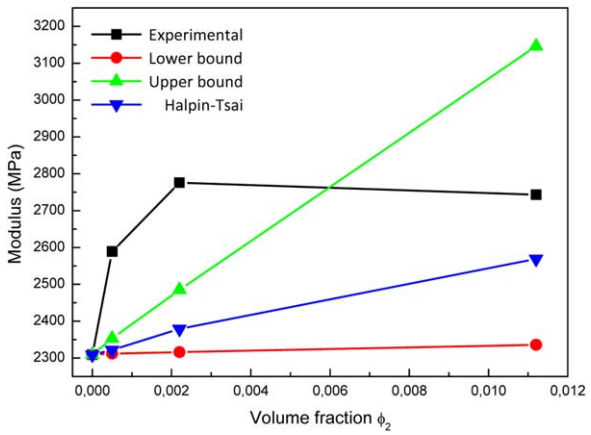

Figure 5. Experimental data and fitting results of PLLA/ZnO nanocomposites as determined by modified Halpin-Tsai model. Fitting results corresponding to the general rule of mixtures are given as a reference. [Color figure can be viewed in the online issue, which is available at wileyonlinelibrary.com.]

Figure 5 shows a comparison between the experimentally obtained data and predicted Young's modulus values according to eq. (3) (note that fitting results corresponding to the general rule of mixtures are given as a reference). It could be noted that the experimental values are higher than the moduli predicted by the fitting models, especially al low concentrations. Indeed, at concentrations up to 0.22v/v % (1 wt %) the Halpin-Tsai underestimates the effective modulus of elasticity of nanocomposites, which suggest a good nanoparticle dispersion and effective stress transfer across the strong ZnO-PLLA interface.[38] However, the modulus is over predicted at high ZnO concentrations as a consequence of the non-homogeneous aggregated nanoparticle dispersion within polymeric matrix (see FE-SEM images). This restriction of segmental mobility of polymeric chains upon uniaxial stress leads to an increase tensile modulus at expenses of elongation at break, as shown in Figure 4. In overall, those results agree well with reported enthalpy relaxation values and electron microscopy images, where it has been found the presence of a critical concentration of 1 wt % in which ZnO nanoparticles are more effective as reinforcing elements.

Dynamic strain−sweep experiments were conducted with the aid of DMA to determine the upper bound of aged materials linear stress−strain regime. Figure 6(a) shows the variation of storage moduli of aged PLLA and PLLA/ZnO 1 wt % with increasing strain (note that data are shown in a log-log plot and for clarity normalized E values are shown). It could be seen that the linear viscoelastic region (LVR, the region within the modulus remains independent of imposed strain level) is notably reduced in presence of zinc oxide, which agrees well with the increase in material brittleness upon ZnO loading shown in Figure 4. Moreover, the LVR decreases upon aging from 1.11% to 0.67% for PLLA and from 0.26% to 0.21% for the nanocomposite containing 1 wt %. This may be ascribed to the embrittlement of the material because of the increased chain stiffness,

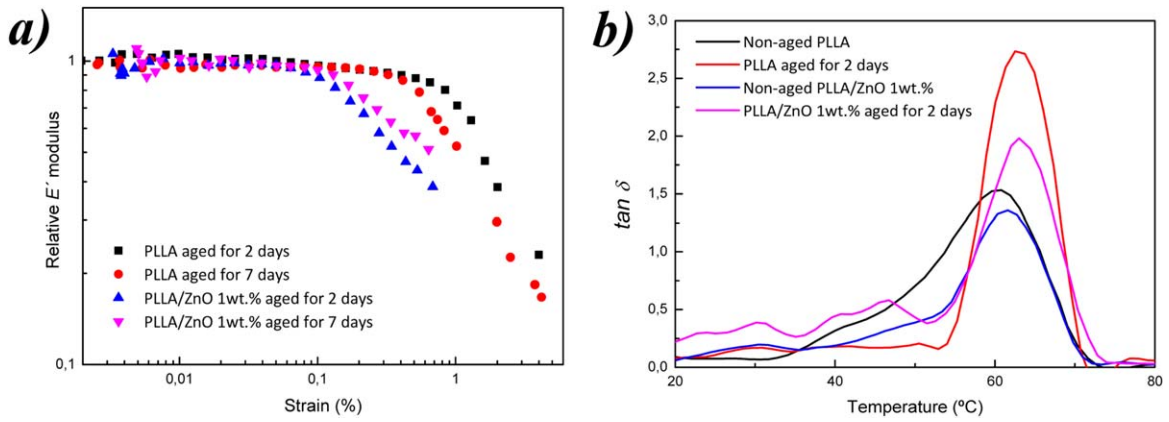

Figure 6. Dynamic strain−sweep (a) and temperature dependence of tan δ (b) of physically aged PLLA and PLLA/ZnO 1 wt %. [Color figure can be viewed in the online issue, which is available at wileyonlinelibrary.com.]

increased density and loss of free volume during physical aging.[7] It should be noticed that for a given aging time, PLLA/ZnO suffers a smaller reduction on the LVR in comparison with neat polymer, indicating slower aging dynamics of PLLA induced by ZnO nanoparticles.[24]

Figure 6(b) depicts the temperature dependence of loss tangent for aged PLLA and its 1 wt % nanocomposite. The maximum of dissipation peak (tan δ) comprised between 55 and 70 °C corresponding to the glass transition of PLLA shifts to higher temperatures and increases its intensity as aging proceeds. The obtained maximum tan δ decreases with ZnO addition as a result of the stiff nature of zinc oxide.[39] Furthermore, the tan δ displacement and height increase results more pronounced for non-reinforced material. For instance, the T_g of neat PLLA from 60.3 °C to 63.1 °C, while for its 1 wt % composite only increases from 61.7 °C to 62.9 °C. Those results further demosntrate that zinc oxide nanoparticles restrict PLLA chain mobility, yielding a reduction in the aging kinetics of the resulting material.

Although performed DSC and FE-SEM experiments indicate that physical aging is notably reduced upon ZnO loading and the extent of this reduction depends on the amount of ZnO-PLLA interfaces, further studies need to be carried out to shed more light on the occurring aging mechanism. In this sense, the analysis of dielectric relaxation behaviour of PLLA/ZnO nanocomposites would be performed in the near future to understand the molecular dynamics and free volume evolution of our materials during the aging process.

CONCLUSIONS

In this work we attempt to reduce the glassy-state structural relaxation of poly (L-lactide) with the addition of well dispersed zinc oxide nanoparticles with no need of surfactant. The aging behavior has been monitored by thermal analysis, where the enthalpy relaxation of nanocomposites as a function of aging time was measured by DSC. Results reveal that physical aging is reduced by a factor of 3.6 with the addition of only 0.25 wt % ZnO nanoparticles, while larger concentrations lead to increased physical aging kinetics. This behavior has been ascribed to the formation of aggregates at concentrations exceeding 1 wt %, which decrease the amount of nanoparticle surfaces exposed to PLLA chains. Furthermore, scanning electron microscopy observations demonstrate that the amount of ZnO-PLLA interfaces is reduced at concentrations ranging from 2 to 5 wt %.

Mechanical tests showed an increased stiffness upon ZnO loading as denoted by the increase in modulus from 2310 MPa to 2780 MPa for the 1 wt % nanocomposite together with a continuous increase in nanocomposite brittleness. The modeling of Youngs modulus carried out according to random Halpin-Tsai equation reveals a good nanoparticle dispersion and effective stress transfer across the ZnO-PLLA interface at low concentrations. Obtained results demonstrate that rod-shaped zinc oxide nanoparticles could serve as effective constraining elements reducing physical aging kinetics of PLLA when is used at ambient temperatures. In overall, it is concluded that the amount of ZnO-PLLA interfaces plays a pivotal role in both structural relaxation and mechanical performance of nanocomposites.

ACKNOWLEDGMENTS

E.L. thanks the University of the Basque Country (UPV/EHU) for a postdoctoral fellowship. We gratefully acknowledge Corbion-Purac for the kind donation of PLLA. Authors thank the Basque Country Government for financial support (Ayudas para apoyar las actividades de los grupos de investigación del sistema universitario vasco, IT718-13). Technical and human support provided by SGIker (UPV/EHU, MICINN, GV/EJ, EGEF and ESF) is gratefully acknowledged.

REFERENCES

1. Martina, M.; Hutmacher, D. W. *Polym. Int.* **2007**, *56*, 145.
2. Auras, R.; Harte, B.; Selke, S. *Macromol. Biosci.* **2004**, *4*, 835.
3. Lizundia, E.; Petisco, S.; Sarasua, J. R. *J. Mech. Behav. Biomed. Mater.* **2013**, *17*, 242.
4. del Rio, J.; Etxeberria, A.; Lopez-Rodriguez, N.; Lizundia, E.; Sarasua, J. R. *Macromolecules* **2010**, *43*, 4698.
5. Angell, C. A.; Ngai, K. L.; McKenna, G. B.; McMillan, P. F.; Martin, S. W. *J. Appl. Phys.* **2000**, *88*, 3113.
6. Kurchan, J. *Nature* **2005**, *433*, 222.

7. Pan, P.; Zhu, B.; Inoue, Y. *Macromolecules* **2007**, *40*, 9664.
8. Kim, J. H.; Koros, W. J.; Paul, D. R. *Polymer* **2006**, *47*, 3094.
9. Kim, J. H.; Koros, W. J.; Paul, D. R. *Polymer* **2006**, *47*, 3104.
10. Hongxia, Z.; Lofgren, E. A.; Jabarin, S. A. *J. Appl. Polym. Sci.* **2009**, *112*, 2906.
11. Cowie, J. M. G.; Harris, S.; McEwen, I. *J. Macromolecules* **1998**, *31*, 2611.
12. Boucher, V. M.; Cangialosi, D.; Alegria, A.; Colmenero, J. *Macromolecules* **2010**, *43*, 7594.
13. Koh, Y. P.; Grassia, L.; Simon, S. L. *Thermochim. Acta* **2015**, *603*, 135.
14. Delpouve, N.; Arnoult, M.; Saiter, A.; Dargent, E.; Saiter, J. M. *Polym. Eng. Sci.* **2014**, *54*, 1144.
15. Lee, A.; Liechtenhan, J. D. *Macromolecules* **1998**, *31*, 4970.
16. Lu, H.; Nutt, S. *Macromol. Chem. Phys.* **2003**, *204*, 1832.
17. Priestley, R. D.; Ellison, C. J.; Broadbelt, L. J.; Torkelson, J. M. *Science* **2005**, *56*, 145.
18. Werner, F.; Gnichwitz, J. F.; Marczak, R.; Palomares, E.; Peukert, W.; Hirsch, A.; Guldi, D. M. *J. Phys. Chem. B* **2010**, *114*, 14671.
19. Lizundia, E.; Ruiz-Rubio, L.; Vilas, J. L.; León, L. M. *J. Appl. Polym. Sci.* **2016**, *133*, DOI: 10.1002/app.42426.
20. Lizundia, E.; Vilas, J. L.; León, L. M. *Carbohydr. Polym.* **2015**, *123*, 256.
21. Struik, L. C. E. *Polymer* **1987**, *28*, 1521.
22. Fischer, E. W.; Sterzel, H. J.; Wegner, G. *Kolloid-Zu Z-Polym.* **1973**, *251*, 980.
23. Hutchinson, J. M.; Smith, S.; Horne, B.; Gourlay, G. M. *Macromolecules* **1999**, *32*, 5046.
24. Lizundia, E.; Sarasua, J. R. *Macromol. Symp.* **2012**, *321*, 118.
25. Boucher, V. M.; Cangialosi, D.; Alegria, A.; Colmenero, J.; Gonzalez-Irun, J.; Liz-Marzan, L. M. *Soft Matter* **2010**, *6*, 3306.
26. Boucher, V. M.; Cangialosi, D.; Alegria, A.; Colmenero, J.; Pastoriza-Santos, I.; Liz-Marzan, L. M. *Soft Matter* **2011**, *7*, 3607.
27. Lin, Y.; Liu, L.; Cheng, J.; Shangguan, Y.; Yu, W.; Qui, B.; Zheng, Q. *RSC Adv.* **2014**, *4*, 20086.
28. Zhiltsov, A.; Gritsenko, O.; Kazakova, V.; Gorbatsevitch, O.; Bessonova, N.; Askadskii, A.; Serenko, O.; Muzafarov, A. *J. Appl. Polym. Sci.* **2015**, *132*, 41894.
29. Liu, M.; Pu, M.; Ma, H. *Compos. Sci. Technol.* **2012**, *72*, 1508.
30. Benali, S.; Aouadi, S.; Dechief, A. L.; Murariu, M.; Dubois, P. *Nanocomposites* **2015**, *1*, 51.
31. Koval'chuk, A. A.; Shchegolikhin, A. N.; Shevchenko, V. G.; Nedorezova, P. M.; Klyamkina, A. N.; Aladyshev, A. M. *Macromolecules* **2008**, *41*, 3149.
32. Cheng, B.; Samulski, E. T. *Chem. Commun.* **2004**, *10*, 986.
33. Murariu, M.; Doumbia, A.; Bonnaud, L.; Dechief, A. L.; Paint, Y.; Ferreira, M.; Campagne, C.; Devaux, E.; Dubois, P. *Biomacromolecules* **2011**, *5*, 1762.
34. Halpin, J. C.; Kardos, J. L. *Polym. Eng. Sci.* **1976**, *16*, 344.
35. Hui, C. Y.; Shia, D. *Polym. Eng. Sci.* **1998**, *38*, 774.
36. Sawai, D.; Tsugane, Y.; Tamada, M.; Kanamoto, T.; Sungil, M.; Hyon, S. *J. Polym. Sci. Part. B: Polym. Phys.* **2007**, *45*, 2632.
37. Kim, H.; Jung, U. S.; Kim, S. I.; Yoon, D.; Cheong, H.; Lee, C. W.; Lee, S. W. *Curr. Appl. Phys.* **2014**, *14*, 166.
38. Choudhury, A. *RSC Adv.* **2014**, *4*, 8856.
39. Lizundia, E.; Urruchi, A.; Vilas, J. L.; León, L. M. *Carbohydr. Polym.* **2016**, *136*, 250.